This article has been accepted for publication in a future issue of this journal, but has not been fully edited. Content may change prior to final publication. Citation information: DOI 10.1109/TEC.2019.2921625, IEEE Transactions on Energy Conversion

Optimal SuDoKu Reconfiguration Technique for Total-Cross-Tied PV array to Increase Power Output Under Non-Uniform Irradiance

Sai Krishna G, Tukaram Moger, *Senior Member, IEEE,*

***Abstract*—Partial Shading Condition drastically reduces the maximum power output of Photovoltaic array. Partial shading occurs due to several factors such as; flying birds, trees and passing clouds, etc. Many ways can be mitigated partial shading problems in PV array. One among the way is reconfiguration techniques, namely reconfigure the location of PV modules in PV array based on irradiance levels in order to distribute shading effects and increasing maximum power. This paper proposed an optimal SuDoKu reconfiguration pattern for 9×9 Total-Cross-Tied PV array to improve maximum power under partial shading conditions. In this approach, the physical location of PV modules in TCT array are rearranged based on optimal SuDoKu style without altering the electrical connections, so that the shading effects can distribute over the array. Further, the performance of proposed pattern investigated with existing SuDoKu pattern under different shading conditions by comparing the Global Maximum Power Point, Mismatch Losses, Fill-Factor and Efficiency using Matlab-Simulink. Based on the results of this paper, it concluded that the proposed optimal SuDoKu reconfiguration arrangement is reducing the line losses and disperse the shading effects over the array as compared to SuDoKu arrangement.**

***Index Terms*—Photovoltaic Modelling, Partial Shading Condition, SuDoKu Pattern, and TCT PV array.**

I. Introduction

NOwadays, the consumers are demanding continuous power supply across the globe. Several factors cause a disturbance in the conventional power system such as a lack of fuel, load shedding, internal failures, and many others. Therefore, the integration of renewable sources become more popular, and their duties are to meet the global demand [1],[2]. The renewable sources are such as solar, wind, geothermal and biomass, etc. The abundant availability of solar energy is one of the best alternative energy and is gaining an immense response from consumers. The output power of PV modules is affected by several factors such as; changes in solar irradiance (G) and temperature (T), variations in series and shunt resistance, soiling and partial shading [3],[4]. Among all, the effect of partial shading diminishes the maximum power output of PV modules. Partial shading occurs if a small part of the PV array shaded due to passing clouds, trees, flying birds and adjacent buildings. In PSC, some part of PV modules may get less intensity of solar irradiance as compared to unshaded part, thus creates a hot-spot effect in PV array. This situation can be avoided by connecting bypass diodes across the PV modules. The inclusion of bypass diodes exhibits multiple steps in I-V and multiple peaks in P-V characteristics of the array. Among all, there is only one global peak which produces the highest maximum power, also known as global maximum power point(GMPP)[5].

The power loss as a result of partial shading dictated by choice of PV array configuration, type of shading pattern and physical location of the PV modules in PV array. Among all, the effect of PV array configuration shows sever impact on maximum power output. Therefore, choosing the right configuration is necessary under PSCs. Various PV array configurations are reported in the literature to reduce mismatch losses caused by partial shadings such as "simple-series (SS), parallel (P), series-parallel (SP), total-cross-tied (TCT), bridge-link (BL) and honey-comb (HC)" [6], [7]. In [8], SP, TCT, and BL PV array configurations are considered for reliability assessment using probabilistic approach under mismatch effects due to manufacturing tolerance. This paper mentioned that TCT and BL PV array configurations are increasing the reliability as compared to SP configured PV array. In [9], partial shading analysis on different PV array configurations such as "SS, SP, TCT, BL, and HC" has been presented. In this work, various parameters such as; maximum power, mismatch losses, and fill-factor are considered to evaluate the performance of each configuration. The obtained result shows that the TCT PV array is reducing the mismatch losses as compared to other PV array configurations. Therefore, as per the literature, TCT PV array is showing less susceptibility to PSCs and producing the highest maximum power as compared to the other configurations [10],[11]. Whereas, the major issues with the TCT configuration is that if the number of PV modules are shaded in a row, that limits the output current of an array [12]. However, to solve this issue, many authors have been proposed reconfiguration techniques for TCT PV array to distribute shading effects from one row to different rows to reduce mismatch losses under PSCs [13],[14].

Based on the literature, these techniques can be classified into dynamic and static reconfiguration techniques. In dynamic technique, PV modules are reconfigured dynamically within the PV array to increase maximum power output under PSCs. In [15], [16], an Electrical Array Reconfiguration (EAR) controller is developed to change the connections between among the PV modules based on irradiance levels for providing input current to the motor. This approach is also employed for an electric car to improve the performance at different driving states such as initial, acceleration, and high-speed [17]. In

The authors are with the Department of Electrical and Electronics Engineering, National Institute of Technology Karnataka, Mangalore, INDIA, 575025 e-mail: {tukaram@nitk.edu.in}

This article has been accepted for publication in a future issue of this journal, but has not been fully edited. Content may change prior to final publication. Citation information: DOI 10.1109/TEC.2019.2921625, IEEE Transactions on Energy Conversion

this paper, the fuzzy logic controller is applied to choose the EAR automatically according to driving states. In [18], a new adaptive PV cell array technique is proposed to reduce PSCs. It consists of a fixed part, adaptive part, and switching matrix. In this technique, the switching matrix plays a crucial role to connect adaptive PV cells into the fixed cells to compensate irradiance drop in each row. An electrical reconfiguration technique [19] is proposed in which the connections of the modules are dynamically changed according to a switching matrix so as to maximize the current of the single string in the event of shading. Though the power loss is reduced under several partial shaded conditions, the technique involves high cost and greater complexity. Still, various papers [18],[13],[20] dealt with the dynamic reconfiguration approach for improving maximum power under partial shading problems. As per the literature, the dynamic reconfiguration technique requires a monitoring system to monitor the shading and faulty PV modules, reconfiguration algorithm for choosing the optimal configuration and switching matrix to make the connections between PV modules. As a result of that, the cost of the dynamic reconfiguration technique would increase. Moreover, the configuration of the system becomes complex [13],[21].

Static reconfigurations utilize a fixed interconnection scheme to improve the power output under partial shading conditions. These do not dynamically change the module position, i.e. the module position is fixed for all shading conditions. This technique doesn't require any sensors, reconfiguration algorithm, and switching matrix as in case of dynamic technique. However, this technique needs an effective reconfigurable pattern for re-arranging the PV modules to distribute shading effects over the array. In [22], they proposed a novel interconnection scheme to distribute partial shading effect. In this approach, the electrical connection between PV modules are made after renumbering. This scheme implemented on 3×3 array, and the result shows that the proposed scheme display superior performance than "SP, TCT, and BL" configured PV arrays. A similar approach is presented [23] to enhance maximum power under PSCs. In [24], a magic square PV array arrangement is developed for 4×4 TCT array to distribute PSCs. During this study, it observed that the proposed arrangement is increasing the output power and reducing the power loss as compared to existing PV array configurations. Consequently, authors [25],[26],[27] proposed various pattern arrangements based on the mathematical approach to distribute PSCs.In [28], a one-time physical arrangement of PV modules connected in a TCT PV array is proposed to enhance the power generation under partial shading conditions. Based on the 9×9SuDoKu puzzle pattern, the modules are physically placed without changing their electrical connection. This arrangement distributes the shading impact across the array, thus improving the PV energy produced. In this approach, the array configured based on a random puzzle pattern and the improvement in power output is obtained for various shading conditions. In this paper, various parameters such as line losses and the dispersion of shade are haven't considered for the study. The line losses depending on the length of the wire required for the connection of SuDoKu arrangement. The measure of shading dispersion depends on the ability of the pattern to disperse any shade to the maximum possible number of rows to minimize the shading effect.

This research describes the creation and formulation of an optimal SuDoKu [28] pattern to decrease line losses and boost shade dispersion for enhanced energy production. In this strategy, the physical location of PV modules in the TCT array is rearranged without changing their electrical connections based on ideal SuDoKu way. Further, the performance of the proposed arrangement investigated with TCT and SuDoKu PV array arrangements by comparing the global maximum power point(GMPP), mismatch losses(ML), fill-factor(FF), and efficiency(η) under various shading conditions using MATLAB-SIMULINK.

A SuDoKu arrangement used in [28] is shown in Fig.1. For example, the module 42 (4^{th} row, 2^{nd} column) is physically relocated to the 1^{st} row but the electrical connection remains unaltered in the 4^{th} row as per this arrangement. Shading dispersion is by shifting the PV modules to distinct rows as per the SuDoKu structure, which decreases the likelihood of shaded modules in the same row and thus distributes them throughout the array. It is important to note that this configuration is a fixed one and not dynamically changing; it remains the same for all shading patterns. This method has reduced mismatch losses; however, there are certain drawbacks associated with this method as follows:

- Line losses: PV modules rearrangement improves the wire length needed in each column to interconnect modules. This improves complete wire resistance and cable losses, resulting in an enhanced voltage drop. The extra length of the wire required for each module depends on the relative position of the previous panel and the next panel in the same column [29]. In this respect, the wire length is directly proportional to the arrangement of SuDoKu arrangement.
- Shading Dispersion factor: Any shading pattern dispersion measure can be used to assess the effectiveness of any rearrangement system. Any shade must be spread over the entire array in such a way that each node enters a maximum and equal current. Two requirements must be fulfilled to ascertain this. First, when a shade happens throughout a whole row, all shaded modules in the row need to be spread across different rows so that the current that enters each row is nearly equal and maximum. Any SuDoKu pattern fulfills this requirement by renumbering the array in such a way that each number in a single line is unique and non-repeating. This would disperse each shaded panel in this row into distinct rows. Second, a shade that occurs over a sub-array has to be distributed among as many rows as possible. The number of rows to which the shade can be distributed limits the maximum size of the sub-array(hence, it limited to 3×3). Thus in each sub-array, the row number must be unique so that a shade occurring on that sub-array is dispersed. However not all sub-arrays in this configuration satisfy this criterion. There exist many sub array i.e. 2×2, 3×2, 3×3 that do not have unique row numbers. Some of these are highlighted in Fig.1.

This article has been accepted for publication in a future issue of this journal, but has not been fully edited. Content may change prior to final publication. Citation information: DOI 10.1109/TEC.2019.2921625, IEEE Transactions on Energy Conversion

11	42	53	94	25	76	87	68	39
21	92	73	84	35	66	57	18	49
31	82	63	44	55	16	97	78	29
41	32	13	54	85	96	77	28	69
51	22	93	64	75	46	17	38	89
61	72	83	24	15	36	47	98	59
71	12	23	34	45	56	67	88	99
81	62	43	74	95	26	37	58	19
91	52	33	14	65	86	27	48	79

Fig. 1. SuDoKu Puzzle pattern [28]

The further Sections of the paper are as follows: Section II, Presents mathematical modelling of a PV module. In Section III, formation of Optimal SuDoKu puzzle and pattern arrangement are discussed. Section III-B, Description of partial shading conditions are considered in this paper. In Section IV, Result and discussions for optimal SuDoKu arrangement under different shading conditions are summarized and followed by the conclusion is presented in Section V.

II. Mathematical modelling of PV Module

Modelling is the first step for analysing the behaviour of PV system. In fact, good and accurate mathematical models are necessary to achieve operation at the optimum point under partial shadings [30]. The modelling of PV module starts with mathematical model of a single PV cell. Many PV cell models have been reported in the literature [31]. Two of them are one diode PV cell and two diode PV cell models. As it is mentioned in the literature, the one diode PV cell model requires less computational efforts as compared to the two diode model [32]. Hence, many researchers are widely using one diode PV cell model because it is very easy to model as compared to other models. The single diode PV cell model ideal, simplified and practical diagram is shown in Fig.2. However, this paper consider practical PV cell for the study.

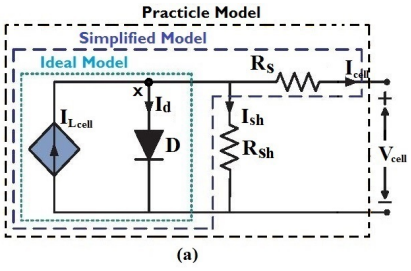

Fig. 2. Equivalent circuit of a PV cell

By applying Kirchhoff's Current Law (KCL) to node 'X' in Fig.2, I_{cell} can be written as,

$$I_{cell} = I_{L,cell} - I_d - I_{sh} \tag{1}$$

where $I_{L,cell}$ is light generated current of the PV cell, I_d is diode current and I_{sh} is a shunt current. The I-V characteristics equation for the PV cell [33] given in Eq.(2);

$$I_{cell} = I_{L,cell} - I_o[exp\{\frac{q(V_{cell} + I_{cell}R_s)}{kaT_c} - 1\}] - \frac{(V_{cell} + I_{cell}R_s)}{R_{sh}} \tag{2}$$

where I_{cell} and V_{cell} are output current and voltage of the PV cell, K is Boltzmann's constant, a is the Ideality factor, T_c is the operating temperature, q is electron charge, R_s and R_{sh} are series and shunt resistance of the PV cell and I_o is the saturation current. However, to model the complete PV cell requires electrical data as well as physical data. The electrical data is provided by the manufactured companies. The physical data such as R_s, R_{sh}, I_o, a, and $I_{L,cell}$ are evaluated by using iterative approach presented in [33]. PV module composed by connecting number of PV cells in series(n_s). The I-V equation of PV module is given in Eq.(3),

$$I_m = I_L - I_o[exp\{\frac{q(V_m + I_m R_S)}{n_s kaT_c} - 1\}] - \frac{(V_m + I_m R_S)}{R_{SH}} \tag{3}$$

where R_S and R_{SH} are series and shunt resistance of a module, I_L is light generated current of the module, I_m and V_m are output current and voltage of the PV module. The above numerical equations are used to plot I-V and P-V characteristics of a PV module with the help of data sheet parameters presented in Table I.

TABLE I: PV module data sheet parameters [25]

Parameters	Ratings
Rated Power	170 watts
Open-Circuit Voltage (V_{oc})	44.2 volts
Short-Circuit Current (I_{sc})	5.2 amps
Current at MPP (I_{mp})	4.75 amps
Voltage at MPP (V_{mp})	35.8 volts
Number of Cells	72
PV Module Area	62.2inc×31.9inc

A. Total-Cross-Tied PV array Configuration

In TCT, first PV modules are connected in parallel to form rows; then all these rows are combined into series to make a string. The layout of TCT configuration is shown in Fig.3. It consists of 81 PV modules assembled into nine rows and nine columns. In each row nine PV modules are connected in parallel. The voltage across each row is same as open-circuit voltage of a single PV module. The output voltage of the array is equal to the sum of row voltages. The output voltage (V_a) of TCT array can be find by applying Kirchhoff's Voltage Law (KVL) to Fig.3,

$$V_a = \sum_{i=1}^{9} V_{mi} \tag{4}$$

where V_{mi} is refers to the maximum voltage at i^{th} row. PV array current (I_a) is equal to the sum of PV modules

This article has been accepted for publication in a future issue of this journal, but has not been fully edited. Content may change prior to final publication. Citation information: DOI 10.1109/TEC.2019.2921625, IEEE Transactions on Energy Conversion

current which are connected in parallel; this can be calculate by applying KCL to each node in Fig.3,

$$I_a = \sum_{j=1}^{9}(I_{ij} - I_{(i+1)j}) = 0 \qquad i = 1, 2, 3, \ ...9 \qquad (5)$$

where i and j are number of rows and columns of the PV array.

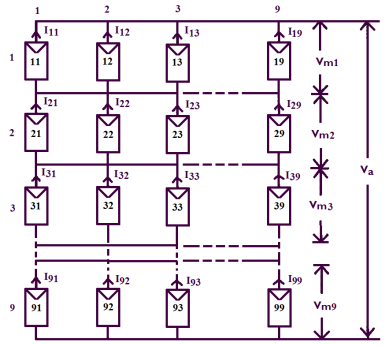

Fig. 3. 9×9 TCT PV Array Configuration

III. Optimal SuDoKu Puzzle and Pattern Arrangement

The necessity for optimizing the SuDoKu configuration to achieve maximum output power is evident and therefore is the main scope of this work. This overcomes the preceding configuration's two primary drawbacks, namely line losses and subarray shadings. Reducing line losses requires a minimum wiring arrangement. The extra wire length needed for each PV module relies on its relative position in the same column in relation to the prior module and next module. Therefore, if the modules are arranged sequentially so that the relative position for most modules is the same as in TCT, the additional wiring is minimized. In addition, an arrangement that disperses the SuDoKu such that each sub-array has unique numbering within itself must be formulated. Thus, a logic sequence is followed to develop the puzzle is illustrated:

- The first column of optimal SuDoKu filled with 1 to 9 numbers in a sequence.
- In order for the next column to be constructed such that each sub-array must have a unique numbering, the numbers in the previous column are shifted by three (max sub-array size). This procedure is followed for the subsequent column also.
- To fill fourth column, the numbers in previous column are shifted by three, but the middle digit replaced by first digit and vice versa.
- In order to fill fifth and sixth column, the numbers in previous column are shifted by three.
- Filling the seventh column is that the numbers in previous column are shifted by three, but the middle digit replaced by first digit and vice versa.
- In order to fill last two columns, the numbers in previous column are shifted by three.

The developed optimal SuDoKu puzzle and pattern arrangement are shown in Figs.4&5. Flowchart for the proposed algorithm to formulate the optimal SuDoKu puzzle is shown in Fig.6. It can be observed from the Fig.5 that there are no sub-arrays of sizes 2×2, 3×2, 2×3, that have non-unique numbering. This is the best possible configuration that can be achieved in any 9×9 SuDoKu pattern. In optimal arrangement, the first digit in the box contains a logic-number and the second digit contains a column. This arrangement is applied to TCT PV array by shifting the physical location of PV modules without altering electrical connections. This enables to distribute the shading modules from same row into entire the array. Hence, the power generated by the PV array is improved for the same shading condition.

1	7	4	2	8	5	3	9	6
2	8	5	3	9	6	1	7	4
3	9	6	1	7	4	2	8	5
4	1	7	5	2	8	6	3	9
5	2	8	6	3	9	4	1	7
6	3	9	4	1	7	5	2	8
7	4	1	8	5	2	9	6	3
8	5	2	9	6	3	7	4	1
9	6	3	7	4	1	8	5	2

Fig. 4. 9×9 Optimal SuDoKu puzzle

11	72	43	24	85	56	37	98	69
21	82	53	34	95	66	17	78	49
31	92	63	14	75	46	27	88	59
41	12	73	54	25	86	67	38	99
51	22	83	64	35	96	47	18	79
61	32	93	44	15	76	57	28	89
71	42	13	84	55	26	97	68	39
81	52	23	94	65	36	77	48	19
91	62	33	74	45	16	87	58	29

Fig. 5. 9×9 Optimal SuDoKu pattern arrangement

A. Wiring Specifications

A 9×9 TCT PV array made up of TSM-170 W Mono crystalline PV modules is considered. The modules are of 170 W power rating and are sized 1.581× 0.809 m^2. The modules in a column are arranged in a continuous fashion. A typical wiring diagram of the PV modules in a column is shown in Fig.7. In Fig.7(a) shows 1^{st} and 2^{nd} column wiring in an arrangement based on SuDoKu. The 2^{nd} column wiring in ideal SuDoKu-based arrangement is shown in Fig.7(b). Each module's present brief circuit Isc is 5.2 A and therefore the wire used to connect the serial components in each column must be 1.56 times Isc (i.e. 7.952) as per the National Electric Code. Hence, 20 AWG wires, which have an ampacity of 7.9 A in enclosed condition, are chosen [33]. These wires have a resistance of 33.3 Ω per km of wire length. Wire spanning the length of one module has a resistance R = 0.0333×1.209 = 0.040 Ω. "In this manner, the resistance of the wires connecting the modules are calculated and the system

This article has been accepted for publication in a future issue of this journal, but has not been fully edited. Content may change prior to final publication. Citation information: DOI 10.1109/TEC.2019.2921625, IEEE Transactions on Energy Conversion

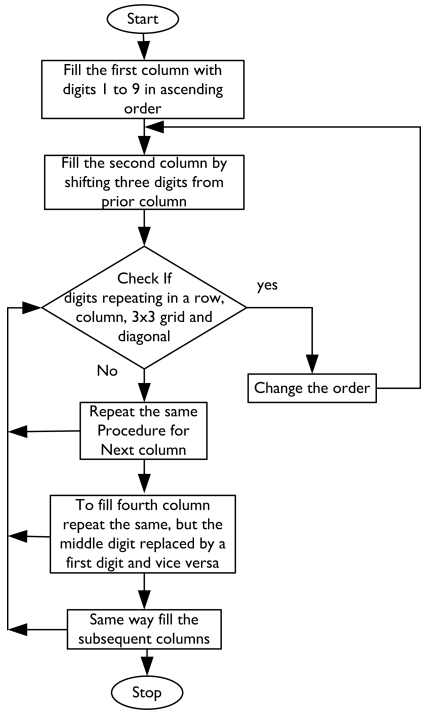

Fig. 6. Flowchart for Optimal SuDoKu puzzle formation

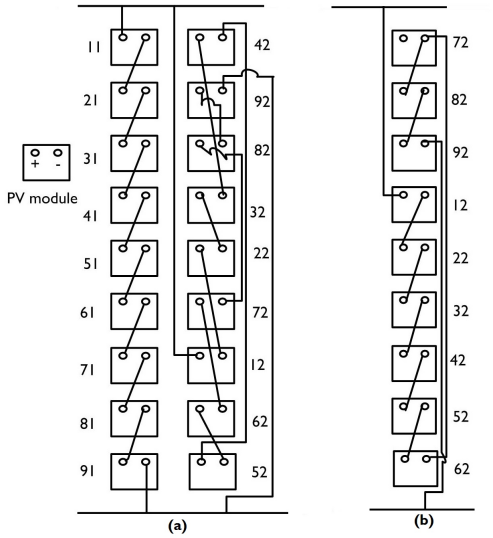

Fig. 7. Wiring diagram for PV array:(a) SuDoKu pattern, (b) Optimal SuDoKu pattern

is modelled in MATLAB/Simulink environment. The circuit connections for a 9×9 TCT array in a SuDoKu arrangement is shown in Fig.8(a)". The circuit connection for a 9×9 TCT array in the proposed optimal SuDoKu arrangement is given in Fig.8(b). "R" is the resistance of a wire spanning the length of one module. The total wire resistance amounts to 281×R for the conventional SuDoKu arrangement whereas it has been optimized to 200×R in the proposed arrangement where the modules are arranged sequentially. The total resistance of the length of the wires used for interconnection remains constant in columns 2 to 9 (25×R) in the proposed scheme. Whereas the corresponding values of wiring resistance is higher and different for columns 2 to 9 in the conventional scheme. The first column is the same in both arrangements and has the least wiring resistance (9×R).

A simple calculation is performed to compute the increase in energy yield due to reduction in line losses. The current at the maximum power point for the specified panel rating is 4.75 A (STC). "The total wire resistance of a SuDoKu configured 9×9 TCT array is (281×R) whereas the total wire resistance of the Optimal SuDoKu configuration is 200×R. Thus the power loss at an uniform irradiance of around 1000 W/m^2 would be $(4.75)^2$ ×(281 R)= 6340.0 W and $(4.75)^2$ ×(200 R)= 4512.04 W respectively". Thus, the proportion of energy saved under STC in the suggested setup owing to decreased wire resistance compared to the previously suggested SuDoKu setup is 28.2%. Assuming an average irradiance of 700-800 W/$m^2$for 8 h a day, it can be calculated that the energy saved is about 110 kWh for a year.

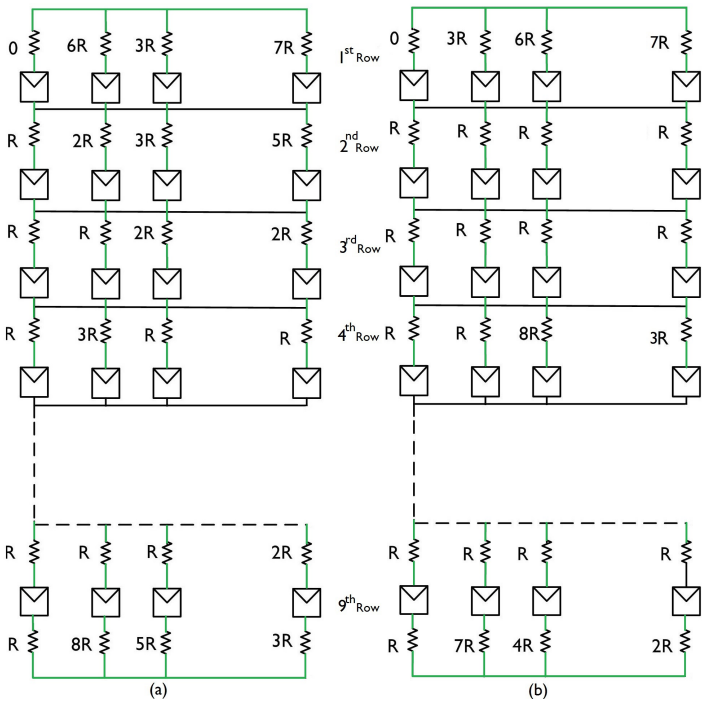

Fig. 8. Circuit connection of 9×9 TCT PV array: (a) SuDoKu arrangement, (b) Optimal SuDoKu arrangement

B. Description of PSCs

In this article, various partial shading conditions are considered to verify the proposed arrangement which are classified into Group-I, Group-II, Group-III, Group-IV, Group-V and Group-VI are shown in Figs.9,11,13,15,17 & 19 respectively. In each group, 4×4 sub-array matrix is subjected to partial shading over 9×9 PV array with different irradiance levels.

This article has been accepted for publication in a future issue of this journal, but has not been fully edited. Content may change prior to final publication. Citation information: DOI 10.1109/TEC.2019.2921625, IEEE Transactions on Energy Conversion

C. Performance Parameters under PSCs

In this section, four parameters are taken into account such as GMPP, ML (%), FF (%) and efficiency (%) to evaluate the performance of proposed arrangement on 9×9 PV array under different shading conditions.

Fill Factor: fill factor (FF) measures the area of PV module or array. The FF can be determine as,

$$FF(\%) = \frac{Power\ at\ GMPP}{V_{oc}.I_{sc}} \tag{6}$$

Mismatch loss: Mismatch loss is the difference between maximum power under normal condition (MPP_{uni}) and global maximum power under PSCs ($GMPP_{PSCs}$). Mismatch loss can be determine as:

$$ML(\%) = \frac{MPP_{uni} - GMPP_{PSCs}}{GMPP_{PSCs}} \tag{7}$$

Efficiency: Efficiency is the ratio of available maximum power output to the solar input. Efficiency can be calculate by,

$$Efficiency(\eta) = \frac{Power\ at\ GMPP}{P_{in}} \tag{8}$$

where P_{in} is solar irradiance falls on the PV array.

IV. Result and Discussions

In this article, an optimal SuDoKu arrangement is proposed for TCT PV array to enhance maximum power output under different shading conditions. Each shading condition, the location of global maximum power point (GMPP) is calculated by theoretically for TCT, SuDoKu [28], optimal SuDoKu arrangements and validated using Matlab/Simulink by comparing the GMPP, ML(%), FF(%) and η(%).

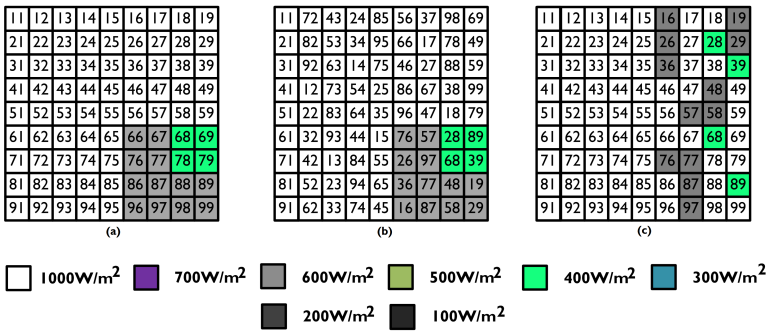

Fig. 9. Group-I shading; (a) TCT PV array arrangement, (b) optimal SuDoKu arrangement, (c) Shading dispersion of optimal SuDoKu arrangement

Group-I Shading: In group-I, the bottom of right corner 4×4 sub-array is subjected to partial shading with various irradiances is shown in Fig.9(a). In this condition, the location of GMPP for TCT, SuDoKu and optimal SuDoKu arrangements are calculated by theoretically.

Location of GMPP for TCT arrangement: To find the location of GMPP, it is necessary to calculate the current generated by each row of the PV array [28]. In $row1$, all PV modules are receiving 1000 W/m^2 irradiance is shown in Fig.9(a).

$$I_{row1} = B_{11}I_{11}+B_{12}I_{12}+B_{13}I_{13}+B_{14}I_{14}+--+B_{19}I_{19} \tag{9}$$

$B_{11} = \frac{G_{11}}{G_o}$=1; where G_{11} is solar irradiance falls on the 11^{th} module in TCT arrangement and I_{11} is current generated by the module 11. Assume that current generated by the each module at Standard Test Condition (STC) is I_m. Therefore, the current generated by the $row1$ is,

$$I_{row1} = 9\times I_m \tag{10}$$

All PV modules in $row2$, $row3$, $row4$ and $row5$ are receiving uniform irradiance 1000 W/m^2. So that, the current generated by all rows,

$$I_{row2} = I_{row3} = I_{row4} = I_{row5} = 9I_m \tag{11}$$

In $row6$ and $row7$, the first five PV modules are receiving 1000 W/m^2 irradiance. Remaining four PV modules, two modules each are receiving 600 W/m^2 and 400 W/m^2 irradiance respectively. The current generated by the $row6$ and $row7$,

$$I_{row6} = I_{row7} = 5\times I_m + 2\times0.6I_m + 2\times0.4I_m \tag{12}$$

In $row8$ and $row9$, the last four PV modules are receiving 600 W/m^2 irradiance and rest of the modules are receiving 1000 W/m^2 irradiance. The current generated by the $row8$ and $row9$ is,

$$I_{row8} = I_{row9} = 5\times I_m + 4\times0.6I_m \tag{13}$$

Since the current generated in different rows is different, there exist multiple peaks on the PV characteristics. Now to identify the location of GMPP, the module currents are noted in Table II according to the order in which panels will be bypassed. Neglecting the small variations in voltage across each row, the voltage of the array V_a = 9 $\times$ V_m,if none of the panels are bypassed and V_a = 8V_m + V_d, where V_d is the voltage across the diode if a single row is bypassed. As $V_d \ll V_a$, V_d is neglected [28].

Power produced by the PV array,

$$P_a = V_a.I_m = 9V_m.I_m \tag{14}$$

The obtained current,voltage and corresponding power for TCT arrangement is noted in Table II. The location of GMPP for optimal SuDoKu arrangement is calculated as follows,

Location of GMPP for optimal SuDoKu arrangement: Optimal SuDoKu arrangement enable to distribute the shading effects over the array under same shading condition is shown in Fig.9(c). The current generated by each row calculated as follows,

In $row1$, $row5$ and $row7$, only two PV modules are receiving 600 W/m^2 irradiance and rest of the modules are receiving 1000 W/m^2 irradiance. The current generated by all rows,

$$I_{row1} = I_{row5} = I_{row7} = 7\times I_m + 2\times0.6I_m \tag{15}$$

This article has been accepted for publication in a future issue of this journal, but has not been fully edited. Content may change prior to final publication. Citation information: DOI 10.1109/TEC.2019.2921625, IEEE Transactions on Energy Conversion

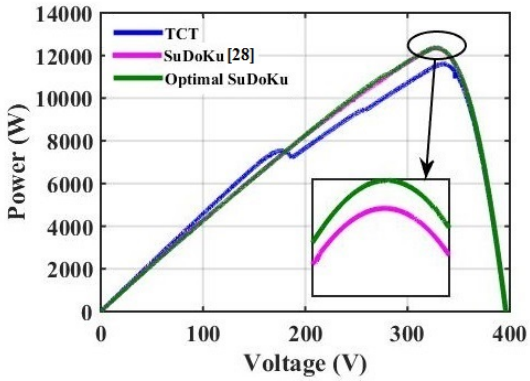

Fig. 10. P-V characteristics for Group-I shading

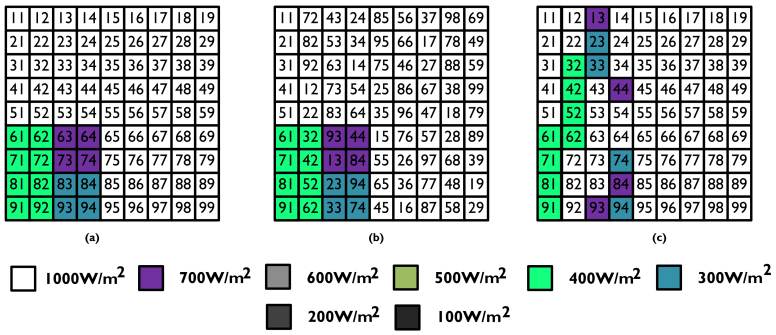

Fig. 11. Group-II shading ; (a) TCT arrangement, (b) optimal SuDoKu arrangement, (c) Shading dispersion of optimal SuDoKu arrangement

In $row3$ and $row8$, two PV modules are receiving 600 W/m^2 and 400 W/m^2 irradiance and rest of the PV modules are receiving 1000 W/m^2 irradiance. The current generated by $row3$ and $row8$,

$$I_{row3} = I_{row8} = 7 \times I_m + 0.6I_m + 0.4I_m \quad (16)$$

In $row4$, $row6$ and $row9$, only one PV module is shaded and rest of the PV modules are receiving 1000 W/m^2 irradiance. The current generated by all rows,

$$I_{row4} = 8 \times I_m + 0.6I_m \quad (17)$$

$$I_{row6} = 8 \times I_m + 0.4I_m \quad (18)$$

$$I_{row9} = 8 \times I_m + 0.6I_m \quad (19)$$

In $row2$, three PV modules are shaded and rest of the PV modules are receiving 1000 W/m^2 irradiance. The current generated by $row2$ is,

$$I_{row2} = 6 \times I_m + 2 \times 0.6I_m + 0.4I_m \quad (20)$$

The obtained current, voltage and corresponding power for optimal SuDoKu arrangement is noted in Table II.

Similarly, the location of GMPP for SuDoKu [28] arrangement is calculated by theoretically under same shading condition is presented in Table II. From the table, it notified that the highest GMPP 68.4 $V_m.I_m$ is produced by the optimal SuDoKu arrangement as compared to the TCT and SuDoKu PV array arrangements. Whereas, the theoretical GMPP validated by plotting the simulated P-V characteristics is shown in Fig.10. Under this condition, the obtained parameters such as GMPP, ML(%), FF(%) and η(%) for all arrangements are graphically represented in Figs.21&22. From the figures, it is clearly observed that the optimal SuDoKu arrangement enhances the global maximum power by 6.5% and 2.1% as compared to TCT and SuDoKu PV array arrangements.

Group-II Shading: In group-II, the bottom of left corner 4×4 sub-array is subjected to partial shading with various irradiances is shown in Fig.11(a).

Location of GMPP for TCT arrangement: In $row1$ to $row5$, all PV modules are receiving uniform irradiance 1000 W/m^2 is shown in Fig.11(a). Current generated by the rows,

$$I_{row1} = I_{row2} = I_{row3} = I_{row4} = I_{row5} = 9 \times I_m \quad (21)$$

In $row6$ and $row7$, first four PV modules, each two are receiving 400 W/m^2 and 700 W/m^2 irradiance. Rest of the five PV modules are receiving 1000 W/m^2 irradiance. The current generated by $row6$ and $row7$ is,

$$I_{row6} = I_{row7} = 5 \times I_m + 2 \times 0.4I_m + 2 \times 0.7I_m \quad (22)$$

In $row8$ and $row9$, first four modules, each two are receiving 400 W/m^2 and 300 W/m^2 irradiance and rest of the PV modules are receiving 1000 W/m^2 irradiance. The current generated by the $row8$ and $row9$ is,

$$I_{row8} = I_{row9} = 5 \times I_m + 2 \times 0.4I_m + 2 \times 0.3I_m \quad (23)$$

The obtained current,voltage and corresponding power for TCT arrangement is noted in Table III.

Similarly, the obtained current, voltage and corresponding power for SuDoKu [28], optimal SuDoKu arrangements under the same shading condition are calculated by theoretically and presented in Table III. From the table, it notified that the highest GMPP of 66.6$V_m.I_m$ is produced by the optimal SuDoKu arrangement as compared to the TCT and SuDoKu arrangements. Whereas, the theoretical GMPP validated by plotting the simulated P-V characteristics is shown in Fig.12. Under this condition, the obtained parameters such as GMPP, ML(%), FF(%) and η(%) for all PV array arrangements are graphically represented in Figs.21&23. From the figures, it is clearly observed that the optimal SuDoKu arrangement enhances the global maximum power by 12.9% and 3.8% as compared to TCT and SuDoKu arrangements.

The same procedure is applied to other shading conditions to find the location of GMPP.

Group-III Shading: In group-III, the top most right corner 4×4 sub-array is subjected to partial shading with different irradiances is shown in Fig.13(a). The location of GMPP for TCT, SuDoKu [22] and optimal SuDoKu arrangements are calculated by theoretically and presented in Table IV. From the table, it notified that the highest GMPP 61.2$V_m.I_m$ is produced

This article has been accepted for publication in a future issue of this journal, but has not been fully edited. Content may change prior to final publication. Citation information: DOI 10.1109/TEC.2019.2921625, IEEE Transactions on Energy Conversion

TABLE II: Location of GMPP for TCT, SuDoKu [28] and Optimal SuDoKu arrangements under group-I shading condition

TCT arrangement				SuDoKu arrangement [28]				Optimal SuDoKu arrangement			
Row bypassed	currents (I_a)	voltages (V_a)	power(P_a)	Row bypassed	currents (I_a)	voltages (V_a)	power(P_a)	Row bypassed	currents (I_a)	voltages (V_a)	power(P_a)
$Irow_9$	$7.4I_m$	$7V_m$	$51.8V_m.I_m$	$Irow_9$	$7.8I_m$	$8V_m$	$62.4V_m.I_m$	$Irow_9$	$8.6I_m$	$2V_m$	$17.2V_m.I_m$
$Irow_8$	$7.4I_m$	-	-	$Irow_8$	$8I_m$	$7V_m$	$56V_m.I_m$	$Irow_8$	$8I_m$	$8V_m$	$64V_m.I_m$
$Irow_7$	$7I_m$	$9V_m$	$\mathbf{63}V_m.I_m$	$Irow_7$	$8.6I_m$	$3V_m$	$25.8V_m.I_m$	$Irow_7$	$8.2I_m$	$6V_m$	$49.2V_m.I_m$
$Irow_6$	$7I_m$	-	-	$Irow_6$	$8.6I_m$	-	-	$Irow_6$	$8.4I_m$	$3V_m$	$25.2V_m.I_m$
$Irow_5$	$9I_m$	$5V_m$	$45V_m.I_m$	$Irow_5$	$7.3I_m$	$9V_m$	$\mathbf{65.7}V_m.I_m$	$Irow_5$	$8.2I_m$	$6V_m$	$49.2V_m.I_m$
$Irow_4$	$9I_m$	-	-	$Irow_4$	$8.2I_m$	$6V_m$	$49.2V_m.I_m$	$Irow_4$	$8.6I_m$	$2V_m$	$17.2V_m.I_m$
$Irow_3$	$9I_m$	-	-	$Irow_3$	$8.2I_m$	-	-	$Irow_3$	$8I_m$	$8V_m$	$64V_m.I_m$
$Irow_2$	$9I_m$	-	-	$Irow_2$	$8.2I_m$	-	-	$Irow_2$	$7.6I_m$	$9V_m$	$\mathbf{68.4}V_m.I_m$
$Irow_1$	$9I_m$	-	-	$Irow_1$	$8.6I_m$	$3V_m$	$25.8V_m.I_m$	$Irow_1$	$8.2I_m$	$6V_m$	$49.2V_m.I_m$

TABLE III: Location of GMPP for TCT, SuDoKu [28] and Optimal SuDoKu arrangements under group-II shading condition

TCT arrangement				SuDoKu arrangement [28]				Optimal SuDoKu arrangement			
Row bypassed	currents (I_a)	voltages (V_a)	power(P_a)	Row bypassed	currents (I_a)	voltages (V_a)	power(P_a)	Row bypassed	currents (I_a)	voltages (V_a)	power(P_a)
$Irow_9$	$6.4I_m$	$9V_m$	$\mathbf{57.6}V_m.I_m$	$Irow_9$	$8.4I_m$	$3V_m$	$25.2V_m.I_m$	$Irow_9$	$7.4I_m$	$9V_m$	$66.6V_m.I_m$
$Irow_8$	$6.4I_m$	-	-	$Irow_8$	$8I_m$	$6V_m$	$48V_m.I_m$	$Irow_8$	$8.1I_m$	$5V_m$	$40.5V_m.I_m$
$Irow_7$	$7.2I_m$	$7V_m$	$50.4V_m.I_m$	$Irow_7$	$7.8I_m$	$8V_m$	$62.4V_m.I_m$	$Irow_7$	$7.7I_m$	$7V_m$	$53.9V_m.I_m$
$Irow_6$	$7.2I_m$	-	-	$Irow_6$	$7.8I_m$	-	-	$Irow_6$	$7.8I_m$	$6V_m$	$46.8V_m.I_m$
$Irow_5$	$9I_m$	$5V_m$	$45V_m.I_m$	$Irow_5$	$8.4I_m$	$3V_m$	$25.2V_m.I_m$	$Irow_5$	$8.4I_m$	$2V_m$	$16.8V_m.I_m$
$Irow_4$	$9I_m$	-	-	$Irow_4$	$8.3I_m$	$4V_m$	$33.2V_m.I_m$	$Irow_4$	$8.1I_m$	$5V_m$	$40.5V_m.I_m$
$Irow_3$	$9I_m$	-	-	$Irow_3$	$8I_m$	$6V_m$	$48V_m.I_m$	$Irow_3$	$7.4I_m$	$9V_m$	$\mathbf{66.6}V_m.I_m$
$Irow_2$	$9I_m$	-	-	$Irow_2$	$8.4I_m$	$3V_m$	$25.2V_m.I_m$	$Irow_2$	$8.3I_m$	$3V_m$	$24.9V_m.I_m$
$Irow_1$	$9I_m$	-	-	$Irow_1$	$7.3I_m$	$9V_m$	$\mathbf{65.7}V_m.I_m$	$Irow_1$	$9I_m$	V_m	$9V_m.I_m$

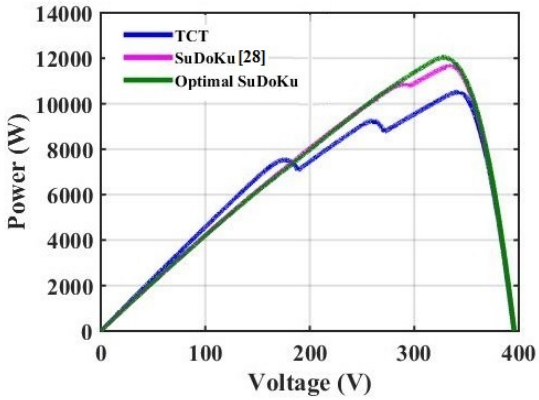

Fig. 12. P-V characteristics for Group-II shading

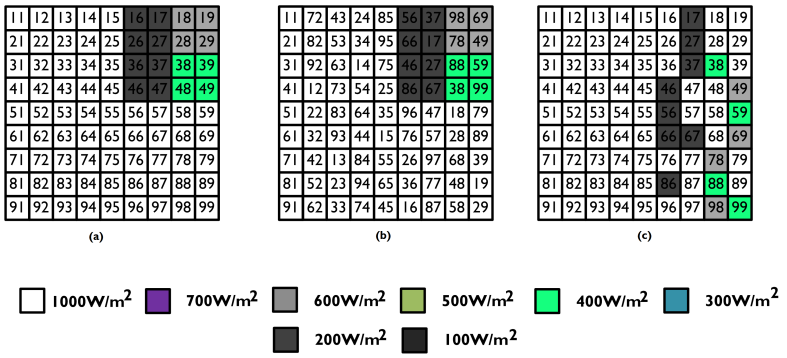

Fig. 13. Group-III shading;(a) TCT arrangement, (b) optimal SuDoKu arrangement, (c) Shading dispersion of optimal SuDoKu arrangement

by the optimal SuDoKu arrangement as compared to TCT and SuDoKu arrangements. Whereas, the theoretical GMPP validated by plotting the simulated P-V characteristics is shown in Fig.14. Under this condition, the obtained parameters such as GMPP, ML(%), FF(%) and η(%) for all PV array arrangements are graphically represented in Figs.21&24.From the figures, it is clearly observed that the optimal SuDoKu arrangement enhances the global maximum power by 9.9% and 1.01% as compared to TCT and SuDoKu PV array arrangements.

Group-IV Shading: Group-IV, top most left corner 4×4 sub-array is subjected to partial shading with different irradiances as shown in Fig.15(a). The location of GMPP for TCT, SuDoKu and optimal SuDoKu arrangements are calculated by theoretically is given in Table V. From the table, it notified that the highest GMPP $59.4V_m.I_m$ is produced by the optimal SuDoKu arrangement as compared to TCT and SuDoKu arrangements. Whereas, the theoretical GMPP validated by plotting the simulated P-V characteristics is shown in Fig.16. Under this condition, the obtained parameters such as GMPP, ML(%), FF(%) and η(%) for all PV array arrangements are graphically represented in Figs.21&25. From the figures, it is clearly observed that the optimal SuDoKu arrangement enhances the global maximum power by 10.9% and 10.1%

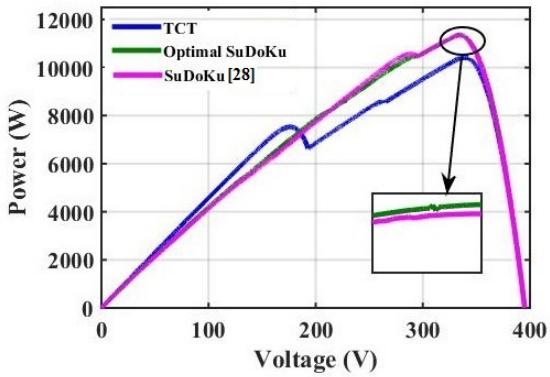

Fig. 14. P-V characteristics for Group-III shading

compared to TCT and SuDoKu PV array arrangements.

Group-V Shading: In group-V, the 4×4 sub-array is subjected to partial shading at the center with different irradiances is shown in Fig.17(a). The location of GMPP for TCT, SuDoKu and optimal SuDoKu arrangement are calculated by theoretically and presented in TableVI. From the table, it is clearly observed that the highest GMPP $64.8V_m.I_m$ is produced by the optimal SuDoKu arrangement as compared

This article has been accepted for publication in a future issue of this journal, but has not been fully edited. Content may change prior to final publication. Citation information: DOI 10.1109/TEC.2019.2921625, IEEE Transactions on Energy Conversion

TABLE IV: Location of GMPP for TCT, SuDoKu [28] and Optimal SuDoKu arrangements under group-III shading condition

TCT arrangement				SuDoKu arrangement [28]				Optimal SuDoKu arrangement			
Row bypassed	currents (I_a)	voltages (V_a)	power(P_a)	Row bypassed	currents (I_a)	voltages (V_a)	power(P_a)	Row bypassed	currents (I_a)	voltages (V_a)	power(P_a)
$Irow_9$	$9I_m$	$5V_m$	$45V_m.I_m$	$Irow_9$	$7.4I_m$	$8V_m$	$59.2V_m.I_m$	$Irow_9$	$8I_m$	$4V_m$	$32V_m.I_m$
$Irow_8$	$9I_m$	-	-	$Irow_8$	$8.2I_m$	$5V_m$	$41V_m.I_m$	$Irow_8$	$7.5I_m$	$8V_m$	$60V_m.I_m$
$Irow_7$	$9I_m$	-	-	$Irow_7$	$6.7I_m$	$9V_m$	$\mathbf{60.3}V_m.I_m$	$Irow_7$	$8.6I_m$	V_m	$8.6V_m.I_m$
$Irow_6$	$9I_m$	-	-	$Irow_6$	$8.2I_m$	$5V_m$	$41V_m.I_m$	$Irow_6$	$6.8I_m$	$9V_m$	$\mathbf{61.2}V_m.I_m$
$Irow_5$	$9I_m$	-	-	$Irow_5$	$8.2I_m$	$5V_m$	$41V_m.I_m$	$Irow_5$	$7.5I_m$	$8V_m$	$60V_m.I_m$
$Irow_4$	$6.2I_m$	$9V_m$	$\mathbf{55.8}V_m.I_m$	$Irow_4$	$8.6I_m$	$2V_m$	$17.2V_m.I_m$	$Irow_4$	$7.7I_m$	$5V_m$	$38.5V_m.I_m$
$Irow_3$	$6.2I_m$	-	-	$Irow_3$	$8.6I_m$	-	-	$Irow_3$	$7.5I_m$	$8V_m$	$60V_m.I_m$
$Irow_2$	$6.6I_m$	$7V_m$	$46.2V_m.I_m$	$Irow_2$	$7.8I_m$	$7V_m$	$54.6V_m.I_m$	$Irow_2$	$8.1I_m$	$3V_m$	$24.3V_m.I_m$
$Irow_1$	$6.6I_m$	-	-	$Irow_1$	$7.8I_m$	-	-	$Irow_1$	$8.1I_m$	$3V_m$	$24.3V_m.I_m$

TABLE V: Location of GMPP for TCT, SuDoKu [28] and Optimal SuDoKu arrangements under group-IV shading condition

TCT arrangement				SuDoKu arrangement [28]				Optimal SuDoKu arrangement			
Row bypassed	currents (I_a)	voltages (V_a)	power(P_a)	Row bypassed	currents (I_a)	voltages (V_a)	power(P_a)	Row bypassed	currents (I_a)	voltages (V_a)	power(P_a)
$Irow_9$	$9I_m$	$5V_m$	$45V_m.I_m$	$Irow_9$	$7.6I_m$	$6V_m$	$45.6V_m.I_m$	$Irow_9$	$8.2I_m$	$2V_m$	$16.4V_m.I_m$
$Irow_8$	$9I_m$	-	-	$Irow_8$	$7.7I_m$	$5V_m$	$38.5V_m.I_m$	$Irow_8$	$8.1I_m$	$3V_m$	$24.3V_m.I_m$
$Irow_7$	$9I_m$	-	-	$Irow_7$	$8.5I_m$	V_m	$8.5V_m.I_m$	$Irow_7$	$7.4I_m$	$8V_m$	$59.2V_m.I_m$
$Irow_6$	$9I_m$	-	-	$Irow_6$	$8.3I_m$	$2V_m$	$16.6V_m.I_m$	$Irow_6$	$8.3I_m$	V_m	$8.3V_m.I_m$
$Irow_5$	$9I_m$	-	-	$Irow_5$	$7.8I_m$	$4V_m$	$31.2V_m.I_m$	$Irow_5$	$7.8I_m$	$4V_m$	$31.2V_m.I_m$
$Irow_4$	$6I_m$	$9V_m$	$\mathbf{54}V_m.I_m$	$Irow_4$	$6.5I_m$	$9V_m$	$\mathbf{58.5}V_m.I_m$	$Irow_4$	$7.7I_m$	$6V_m$	$46.2V_m.I_m$
$Irow_3$	$6I_m$	-	-	$Irow_3$	$7.4I_m$	$8V_m$	$59.2V_m.I_m$	$Irow_3$	$7.7I_m$	$6V_m$	$46.2V_m.I_m$
$Irow_2$	$6.2I_m$	$7V_m$	$43.4V_m.I_m$	$Irow_2$	$8.1I_m$	$3V_m$	$24.3V_m.I_m$	$Irow_2$	$7.6I_m$	$7V_m$	$53.2V_m.I_m$
$Irow_1$	$6.2I_m$	-	-	$Irow_1$	$7.4I_m$	$8V_m$	$59.2V_m.I_m$	$Irow_1$	$6.6I_m$	$9V_m$	$\mathbf{59.4}V_m.I_m$

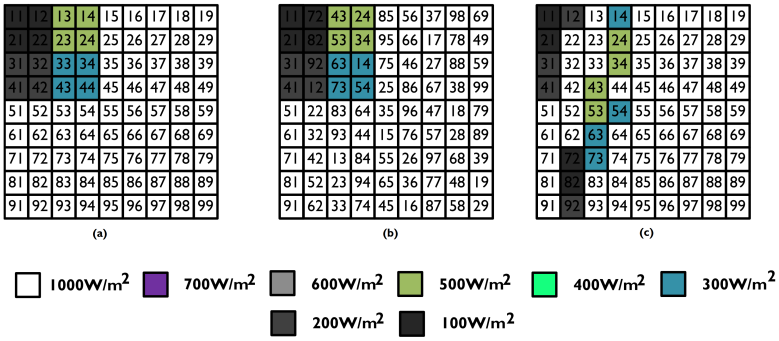

Fig. 15. Group-IV shading ;(a) TCT arrangement, (b) optimal SuDoKu arrangement, (c) Shading dispersion of optimal SuDoKu arrangement

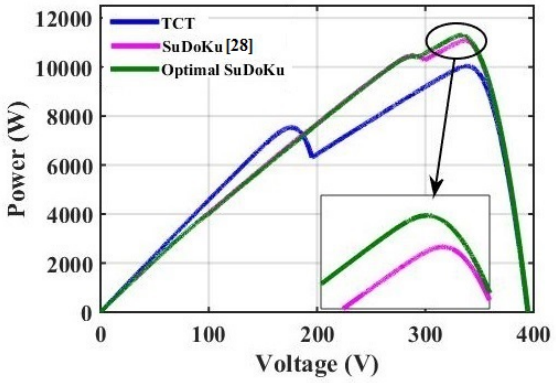

Fig. 16. P-V characteristics for Group-IV shading

to TCT and SuDoKu PV array arrangements. Whereas, the theoretical GMPP validated by plotting the simulated P-V characteristics is shown in Fig.18. Under this condition, the obtained parameters such as GMPP, ML(%), FF(%) and η(%) for all PV array arrangements are graphically represented in Figs.21&26. From the figures, it is clearly observed that the optimal SuDoKu arrangement enhances the global maximum power by 21.6% and 13.9% compared to TCT and SuDoKu PV array arrangements.

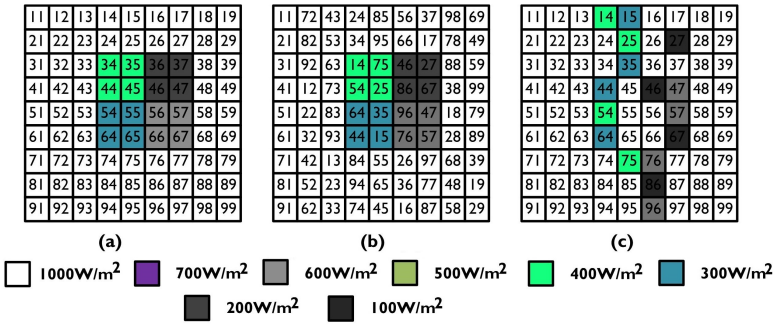

Fig. 17. Group-V shading ;(a) TCT arrangement, (b) optimal SuDoKu arrangement, (c) Shading dispersion of optimal SuDoKu arrangement

Group-VI Shading: In group-VI, two 3×3 sub-arrays are subjected to partial shading at the center with different irradiances is shown in Fig.19(a). The location of GMPP for TCT, SuDoKu and optimal SuDoKu arrangement are calculated by theoretically and presented in Table VII.From the table, it is clearly observed that the highest GMPP $63V_m.I_m$ is produced by the optimal SuDoKu arrangement as compared

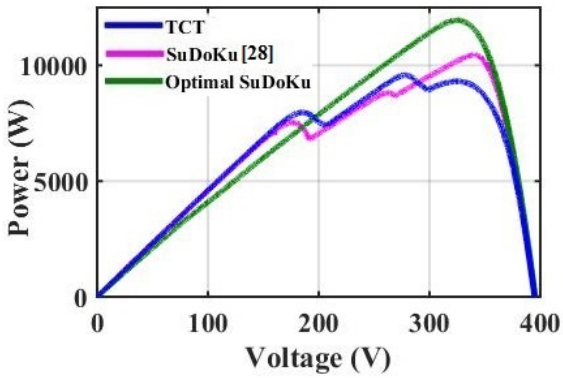

Fig. 18. P-V characteristics for Group-V shading

This article has been accepted for publication in a future issue of this journal, but has not been fully edited. Content may change prior to final publication. Citation information: DOI 10.1109/TEC.2019.2921625, IEEE Transactions on Energy Conversion

TABLE VI: Location of GMPP for TCT, SuDoKu [28] and Optimal SuDoKu arrangements under group-V shading condition

TCT arrangement				SuDoKu arrangement [28]				Optimal SuDoKu arrangement			
Row bypassed	currents (I_a)	voltages (V_a)	power(P_a)	Row bypassed	currents (I_a)	voltages (V_a)	power(P_a)	Row bypassed	currents (I_a)	voltages (V_a)	power(P_a)
$Irow_9$	$9I_m$	$5V_m$	$45V_m.I_m$	$Irow_9$	$6.8I_m$	$9V_m$	**61.2**$V_m.I_m$	$Irow_9$	$8.6I_m$	V_m	$8.6V_m.I_m$
$Irow_8$	$9I_m$	-	-	$Irow_8$	$8.4I_m$	$2V_m$	$16.8V_m.I_m$	$Irow_8$	$8.1I_m$	$3V_m$	$24.3V_m.I_m$
$Irow_7$	$9I_m$	-	-	$Irow_7$	$7.5I_m$	$8V_m$	$60V_m.I_m$	$Irow_7$	$8I_m$	$5V_m$	$40V_m.I_m$
$Irow_6$	$6.8I_m$	$7V_m$	$47.6V_m.I_m$	$Irow_6$	$8.3I_m$	$4V_m$	$33.2V_m.I_m$	$Irow_6$	$7.4I_m$	$8V_m$	$59.2V_m.I_m$
$Irow_5$	$6.8I_m$	-	-	$Irow_5$	$7.8I_m$	$6V_m$	$46.8V_m.I_m$	$Irow_5$	$8I_m$	$5V_m$	$40V_m.I_m$
$Irow_4$	$6.2I_m$	$9V_m$	**55.8**$V_m.I_m$	$Irow_4$	$7.6I_m$	$7V_m$	$53.2V_m.I_m$	$Irow_4$	$7.2I_m$	$9V_m$	**64.8**$V_m.I_m$
$Irow_3$	$6.2I_m$	-	-	$Irow_3$	$8.6I_m$	V_m	$8.6V_m.I_m$	$Irow_3$	$8.3I_m$	$2V_m$	$16.6V_m.I_m$
$Irow_2$	$9I_m$	$5V_m$	$45V_m.I_m$	$Irow_2$	$8.3I_m$	$4V_m$	$33.2V_m.I_m$	$Irow_2$	$7.5I_m$	$7V_m$	$52.5V_m.I_m$
$Irow_1$	$9I_m$	-	-	$Irow_1$	$7.8I_m$	$6V_m$	$46.8V_m.I_m$	$Irow_1$	$7.7I_m$	$6V_m$	$46.2V_m.I_m$

to TCT and SuDoKu PV array arrangements. Whereas, the theoretical GMPP validated by plotting the simulated P-V characteristics is shown in Fig.20. Under this condition, the obtained parameters such as GMPP, ML(%), FF(%) and η(%) for all PV array arrangements are graphically represented in Figs.21&27. From the figures, it is clearly observed that the optimal SuDoKu arrangement enhances the global maximum power by 12.9% and 10.12% compared to TCT and SuDoKu PV array arrangements.

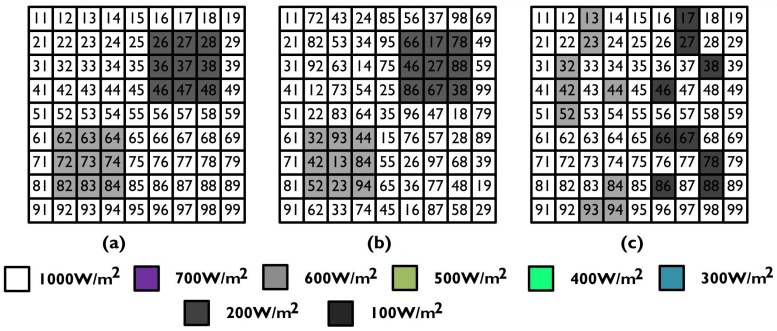

Fig. 19. Group-VI shading ;(a) TCT arrangement, (b) optimal SuDoKu arrangement, (c) Shading dispersion of optimal SuDoKu arrangement

A. Comparative study on existing PV array arrangements

In this section various existing PV array arrangements schemes are considered to reduce mismatch losses under various shading conditions. The basic TCT connection has the maximum mismatch losses as compared to the other configurations. Table VIII shows the power output of TCT, EAR [19], SuDoKu [28] and proposed optimal SuDoKu arrangements

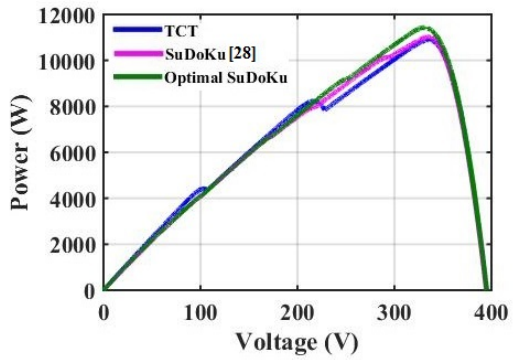

Fig. 20. P-V characteristics for Group-VI shading

for Group-I to Group-IV shading conditions. Electrical array reconfiguration methods that use a switch matrix to dynamically alter the interconnection provide maximum energy output with minimal losses of incompatibility. At different points, voltages and currents are felt to determine the best possible interconnection and regulate the matrix of the switch. However, the SuDoKu methods are based on a static interconnection system that does not dynamically alter the positions of the PV modules. Compared to the TCT interconnection, it provides a significant reduction in mismatch losses. The writers in [28] did not, however, take into consideration the line losses and dispersion factor. So that, in this work an optimized SuDoKu arrangement is developed. This arrangement scheme reduces the line losses as well as mismatch losses due to better dispersion. The losses associated with mismatch are slightly greater than in EAR setup. The distinction between the suggested arrangement's energy inputs and EAR is very tiny. In other words, energy enhancement is very small (around 2.6%). However, this enhancement is accomplished in EAR at the expense of countless sensors, switches and complicated controllers etc. In the proposed arrangement, no such sensors or switches or controllers are essential. However, it must be taken into account that no switches or sensors have been used to implement the proposed technique.

B. Expansion of $m \times n$ array

The formation of a 9×9 optimal SuDoKu pattern has been obtained using the proposed algorithm. However, this algorithm can extended to any size of the array like 16×16, 25×25 etc. This can also reduce the wiring losses and improve the shading dispersion factor under sub-array by choosing m rows and n columns.

The study as mentioned earlier, it is indicated that the optimal SuDoKu arrangement is enhancing the global maximum power as compared to TCT and SuDoKu [28] PV array arrangements under all shading conditions.

V. Conclusion

This paper proposed an optimal SuDoKu arrangement for TCT PV array to increase maximum power output under partial shading condition. In this work, six partial shading conditions are considered. In each condition, the location of global maximum power point is calculated by theoretically and validated using MATLAB/SIMULINK by comparing the GMPP, mismatch loss, fill factor and efficiency. From the results mentioned above, it is observed that the optimal SuDoKu arrangement enhances the global maximum power and reduces

This article has been accepted for publication in a future issue of this journal, but has not been fully edited. Content may change prior to final publication. Citation information: DOI 10.1109/TEC.2019.2921625, IEEE Transactions on Energy Conversion

TABLE VII: Location of GMPP for TCT, SuDoKu [28] and Optimal SuDoKu arrangements under group-VI shading condition

TCT arrangement				SuDoKu arrangement [28]				Optimal SuDoKu arrangement			
Row bypassed	currents (I_a)	voltages (V_a)	power(P_a)	Row bypassed	currents (I_a)	voltages (V_a)	power(P_a)	Row bypassed	currents (I_a)	voltages (V_a)	power(P_a)
$Irow_9$	$9I_m$	$3V_m$	$27V_m.I_m$	$Irow_9$	$7.4I_m$	$7V_m$	$51.8V_m.I_m$	$Irow_9$	$8.2I_m$	$3V_m$	$24.6V_m.I_m$
$Irow_8$	$7.8I_m$	$6V_m$	$46.8V_m.I_m$	$Irow_8$	$8.6I_m$	$3V_m$	$25.8V_m.I_m$	$Irow_8$	$7I_m$	$9V_m$	$\mathbf{63}V_m.I_m$
$Irow_7$	$7.8I_m$	$6V_m$	$46.8V_m.I_m$	$Irow_7$	$6.8I_m$	$9V_m$	$\mathbf{61.2}V_m.I_m$	$Irow_7$	$8.2I_m$	$3V_m$	$24.6V_m.I_m$
$Irow_6$	$7.8I_m$	-	-	$Irow_6$	$7.8I_m$	$5V_m$	$39V_m.I_m$	$Irow_6$	$7.4I_m$	$8V_m$	$59.2V_m.I_m$
$Irow_5$	$9I_m$	$3V_m$	$27V_m.I_m$	$Irow_5$	$8.2I_m$	$4V_m$	$32.8V_m.I_m$	$Irow_5$	$8.6I_m$	V_m	$8.6V_m.I_m$
$Irow_4$	$6.6I_m$	$9V_m$	$\mathbf{59.4}V_m.I_m$	$Irow_4$	$9I_m$	V_m	$9V_m.I_m$	$Irow_4$	$7.4I_m$	$8V_m$	$59.2V_m.I_m$
$Irow_3$	$6.6I_m$	-	-	$Irow_3$	$8.6I_m$	$3V_m$	$25.8V_m.I_m$	$Irow_3$	$7.8I_m$	$6V_m$	$46.8V_m.I_m$
$Irow_2$	$6.6I_m$	-	-	$Irow_2$	$7.4I_m$	$7V_m$	$51.8V_m.I_m$	$Irow_2$	$7.8I_m$	-	-
$Irow_1$	$9I_m$	$3V_m$	$27V_m.I_m$	$Irow_1$	$7I_m$	$8V_m$	$56V_m.I_m$	$Irow_1$	$7.8I_m$	-	-

TABLE VIII: Variation in power output for PV array arrangements under partial shadings

PV arrangement scheme	G-I (W)	G-II (W)	G-III (W)	G-IV (W)
TCT	11590	10500	10360	10038
SuDoKu	12260	11700	11350	11090
Optimal SuDoKu	12390	12050	11390	11190
EAR	12380	12130	11410	11260

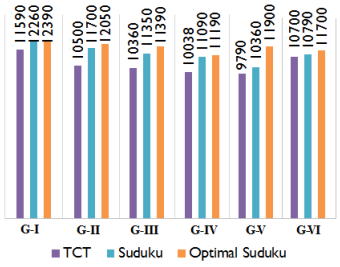

Fig. 21. GMPP for all arrangements under all shading conditions (W)

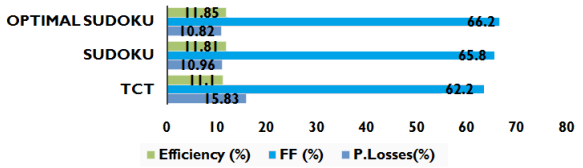

Fig. 22. Mismatch power loss, fill factor and efficiency for Group-I shading condition

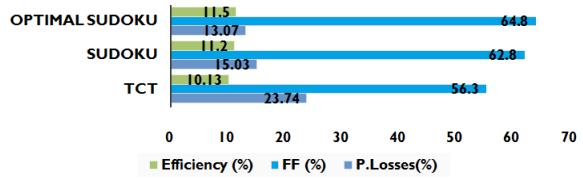

Fig. 23. Mismatch power loss, fill factor and efficiency for Group-II shading condition

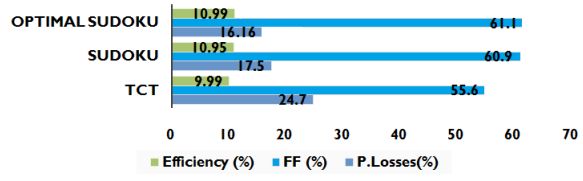

Fig. 24. Mismatch power loss, fill factor and efficiency for Group-III shading condition

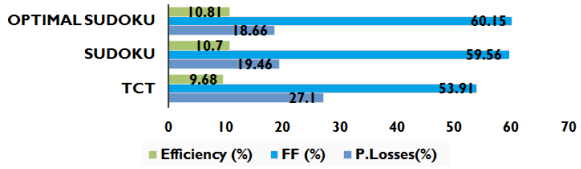

Fig. 25. Mismatch power loss, fill factor and efficiency for Group-IV shading condition

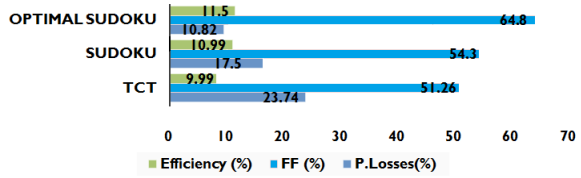

Fig. 26. Mismatch power loss, fill factor and efficiency for Group-V shading condition

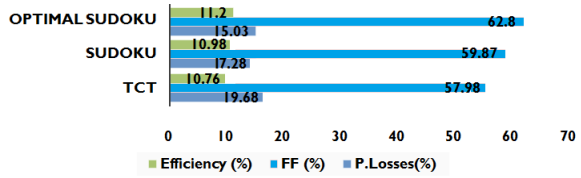

Fig. 27. Mismatch power loss, fill factor and efficiency for Group-VI shading condition

the mismatch losses as compared to TCT and SuDoKu PV array arrangements under all shading conditions.

REFERENCES

[1] Y. Mahmoud and E. F. El-Saadany, "Enhanced reconfiguration method for reducing mismatch losses in pv systems," *IEEE Journal of Photovoltaics*, vol. 7, no. 6, pp. 1746–1754, 2017.

[2] B. Subudhi and R. Pradhan, "A new adaptive maximum power point controller for a photovoltaic system," *IEEE Transactions on Sustainable Energy*, 2018.

[3] A. Mäki and S. Valkealahti, "Power losses in long string and parallel-connected short strings of series-connected silicon-based photovoltaic modules due to partial shading conditions," *IEEE Transactions on Energy Conversion*, vol. 27, no. 1, pp. 173–183, 2012.

TABLE IX: Power enhancement by optimal SuDoKu

Shading cases	Maximum Power Output (W)		Power enhancement(%)
	SuDoKu	Optimal SuDoKu	
Group-I	12260	12390	2.1
Group-II	11700	12050	3.8
Group-III	11350	11390	1.01
Group-VI	11090	11190	10.1
Group-V	11500	12050	13.9
Group-VI	10790	11700	10.12

[4] M. Balato, L. Costanzo, P. Marino, G. Rubino, L. Rubino, and M. Vitelli, "Modified teodi mppt technique: Theoretical analysis and experimental validation in uniform and mismatching conditions," *IEEE Journal of Photovoltaics*, vol. 7, no. 2, pp. 604–613, 2017.

[5] H. Patel and V. Agarwal, "Matlab-based modeling to study the effects of partial shading on pv array characteristics," *IEEE transactions on energy conversion*, vol. 23, no. 1, pp. 302–310, 2008.

[6] Y.-J. Wang and P.-C. Hsu, "An investigation on partial shading of pv modules with different connection configurations of pv cells," *Energy*, vol. 36, no. 5, pp. 3069–3078, 2011.

[7] N. Gautam and N. Kaushika, "Network analysis of fault-tolerant solar photovoltaic arrays," *Solar Energy Materials and Solar Cells*, vol. 69, no. 1, pp. 25–42, 2001.

[8] N. K. Gautam and N. Kaushika, "Reliability evaluation of solar photovoltaic arrays," *Solar Energy*, vol. 72, no. 2, pp. 129–141, 2002.

[9] O. Bingöl and B. Özkaya, "Analysis and comparison of different pv array configurations under partial shading conditions," *Solar Energy*, vol. 160, pp. 336–343, 2018.

[10] S. Bana and R. Saini, "Experimental investigation on power output of different photovoltaic array configurations under uniform and partial shading scenarios," *Energy*, vol. 127, pp. 438–453, 2017.

[11] S. R. Pendem and S. Mikkili, "Modelling and performance assessment of pv array topologies under partial shading conditions to mitigate the mismatching power losses," *Solar Energy*, vol. 160, pp. 303–321, 2018.

[12] M. S. El-Dein, M. Kazerani, and M. Salama, "Optimal photovoltaic array reconfiguration to reduce partial shading losses," *IEEE Transactions on Sustainable Energy*, vol. 4, no. 1, pp. 145–153, 2013.

[13] D. La Manna, V. L. Vigni, E. R. Sanseverino, V. Di Dio, and P. Romano, "Reconfigurable electrical interconnection strategies for photovoltaic arrays: A review," *Renewable and Sustainable Energy Reviews*, vol. 33, pp. 412–426, 2014.

[14] G. Petrone, G. Spagnuolo, Y. Zhao, B. Lehman, C. Ramos, and M. Orozco, "Dynamical reconfiguration for fighting mismatched conditions and meeting load requests," 2015.

[15] Z. M. Salameh and F. Dagher, "The effect of electrical array reconfiguration on the performance of a pv-powered volumetric water pump," *IEEE Transactions on Energy Conversion*, vol. 5, no. 4, pp. 653–658, 1990.

[16] Z. M. Salameh and C. Liang, "Optimum switching points for array reconfiguration controller," pp. 971–976, 1990.

[17] Y. Auttawaitkul, B. Pungsiri, K. Chammongthai, and M. Okuda, "A method of appropriate electrical array reconfiguration management for photovoltaic powered car," pp. 201–204, 1998.

[18] D. Nguyen and B. Lehman, "An adaptive solar photovoltaic array using model-based reconfiguration algorithm," *IEEE Transactions on Industrial Electronics*, vol. 55, no. 7, pp. 2644–2654, 2008.

[19] G. Velasco-Quesada, F. Guinjoan-Gispert, R. Piqué-López, M. Román-Lumbreras, and A. Conesa-Roca, "Electrical pv array reconfiguration strategy for energy extraction improvement in grid-connected pv systems," *IEEE Transactions on Industrial Electronics*, vol. 56, no. 11, pp. 4319–4331, 2009.

[20] K. Ş. Parlak, "Pv array reconfiguration method under partial shading conditions," *International Journal of Electrical Power & Energy Systems*, vol. 63, pp. 713–721, 2014.

[21] G. S. Krishna and T. Moger, "Reconfiguration strategies for reducing partial shading effects in photovoltaic arrays: State of the art," *Solar Energy*, vol. 182, pp. 429 – 452, 2019.

[22] P. S. Rao, G. S. Ilango, and C. Nagamani, "Maximum power from pv arrays using a fixed configuration under different shading conditions," *IEEE journal of Photovoltaics*, vol. 4, no. 2, pp. 679–686, 2014.

[23] M. Jazayeri, K. Jazayeri, and S. Uysal, "Adaptive photovoltaic array reconfiguration based on real cloud patterns to mitigate effects of non-uniform spatial irradiance profiles," *Solar Energy*, vol. 155, pp. 506–516, 2017.

[24] A. S. Yadav, R. K. Pachauri, Y. K. Chauhan, S. Choudhury, and R. Singh, "Performance enhancement of partially shaded pv array using novel shade dispersion effect on magic-square puzzle configuration," *Solar Energy*, vol. 144, pp. 780–797, 2017.

[25] A. S. Yadav, R. K. Pachauri, and Y. K. Chauhan, "Comprehensive investigation of pv arrays with puzzle shade dispersion for improved performance," *Solar Energy*, vol. 129, pp. 256–285, 2016.

[26] R. Pachauri, A. S. Yadav, Y. K. Chauhan, A. Sharma, and V. Kumar, "Shade dispersion-based photovoltaic array configurations for performance enhancement under partial shading conditions," *International Transactions on Electrical Energy Systems*, 2018.

[27] B. Dhanalakshmi and N. Rajasekar, "Dominance square based array reconfiguration scheme for power loss reduction in solar photovoltaic (pv) systems," *Energy Conversion and Management*, vol. 156, pp. 84–102, 2018.

[28] B. I. Rani, G. S. Ilango, and C. Nagamani, "Enhanced power generation from pv array under partial shading conditions by shade dispersion using su do ku configuration," *IEEE Transactions on sustainable energy*, vol. 4, no. 3, pp. 594–601, 2013.

[29] A. S. Yadav and V. Mukherjee, "Line losses reduction techniques in puzzled pv array configuration under different shading conditions," *Solar Energy*, vol. 171, pp. 774–783, 2018.

[30] L. Gao, R. A. Dougal, S. Liu, and A. P. Iotova, "Parallel-connected solar pv system to address partial and rapidly fluctuating shadow conditions," *IEEE Transactions on industrial Electronics*, vol. 56, no. 5, pp. 1548–1556, 2009.

[31] F. Dkhichi, B. Oukarfi, A. Fakkar, and N. Belbounaguia, "Parameter identification of solar cell model using levenberg–marquardt algorithm combined with simulated annealing," *Solar energy*, vol. 110, pp. 781–788, 2014.

[32] K. Yan, Y. Du, and Z. Ren, "Mppt perturbation optimization of photovoltaic power systems based on solar irradiance data classification," *IEEE Transactions on Sustainable Energy*, 2018.

[33] M. G. Villalva, J. R. Gazoli, and E. Ruppert Filho, "Comprehensive approach to modeling and simulation of photovoltaic arrays," *IEEE Transactions on power electronics*, vol. 24, no. 5, pp. 1198–1208, 2009.

Sai Krishna G received the B.Tech degree in electrical & electronics engineering and M.Tech. degree in electrical energy system from JNTU University, Anantapur, Andhra Pradesh, India, in 2010 & 2012 respectively. He is presently pursuing his Ph.D degree in the department of electrical & electronics engineering in National Institute Technology Karnataka Surathkal,India. His research interest includes grid Integration of renewable energy, adaptive solar photovoltaic systems, Isolated and Non-isolated DC-DC converters.

Tukaram Moger (M'10, SM'19) received B.E. degree in electrical and electronics engineering from Karnatak University, Dharwad, Karnataka, India, in 2001, M.Tech. degree in electrical engineering from Indian Institute of Technology Kanpur (IITK), UP, India, in 2005, and Ph.D. degree in electrical engineering from Indian Institute of Science (IISc) Bengaluru, India, in 2016. He has been associated with academic institutions as a faculty member and currently working as assistant professor in the Department of Electrical and Electronics Engineering, National Institute of Technology Karnataka (NITK), Surathkal, Mangaluru, India. His research interests include grid Integration of renewable energy, solar photovoltaic systems, reactive power and voltage control, power system operation and planning, power system deregulation. He is a senior member of IEEE (USA), IEEE Power & Energy Society (PES), member of IEEE Eta-Kappa Nu (Mu Xi Chapter of IISc), IET (UK), CIGRE, Institution of Engineers (India), and life member of Indian Society for Technical Education (ISTE), System Society of India (SSI) and Soft Computing Research Society (SCRS) of India. He also holds Chartered Engineer (India) certificate.